



Ionic liquid (1-butyl-1-methylpyrrolidinium trifluoromethanesulfonate) doped polyethylene polymer electrolyte for energy devices

Suneyana Rawat^{1,*}, Pramod K. Singh^{1,*} , Amrita Jain², Shufeng Song³, M. Z. A. Yahya⁴, Serguei V. Savilov⁵, Markus Diantoro⁶, Monika Michalska⁷, Anji Reddy Polu⁸, and Ram Chandra Singh^{1,*}

¹ Center for Solar Cells and Renewable Energy (CSRE), Department of Physics, SSBSR, Sharda University, Greater Noida 201310, India

² Institute of Fundamental Technological Research, Polish Academy of Sciences, Pawińskiego 5B, 02-106 Warsaw, Poland

³ College of Aerospace Engineering, Chongqing University, Chongqing 400044, People's Republic of China

⁴ Faculty of Defence Science and Technology, Universiti Pertahanan Nasional Malaysia (UPNM), 57000 Kuala Lumpur, Malaysia

⁵ Department of Chemistry, Lomonosov Moscow State University, 1-3 Lenninskiye Gory, Moscow, Russia 119991

⁶ Department of Physics, Faculty of Mathematics and Natural Science, Universitas Negeri Malang, Malang 65145, Indonesia

⁷ Department of Chemistry and Physico-Chemical Processes, Faculty of Materials Science and Technology, VSB-Technical University of Ostrava, 17. listopadu 2172/15, Poruba, 708 00 Ostrava, Czech Republic

⁸ Department of Physics, BVRIT HYDERABAD College of Engineering for Women, Hyderabad, Telangana 500090, India

Received: 24 May 2024

Accepted: 15 August 2024

© The Author(s), under exclusive licence to Springer Science+Business Media, LLC, part of Springer Nature, 2024

ABSTRACT

This paper provides a comprehensive overview of the influence of 1-Butyl-1-Methylpyrrolidinium Trifluoromethanesulfonate (BMPyrrOTf)-ionic liquid on a new polymer electrolyte where Polyethylene oxide (PEO) as host and ammonium iodide (NH₄I) as salt. These IL-doped solid polymer electrolyte were prepared using solution cast technique. Various characterisation techniques have been utilized to evaluate the qualitative and quantitative estimation of polymer electrolyte like Polarized microscopy (POM), X-ray diffraction (XRD), Fourier transform infrared spectroscopy (FTIR), Linear sweep voltammetry (LSV), Ionic transferance no. (t_{ion}) and Impedance spectroscopy. Doping IL increases conductivity and highest achieve at 8 wt% of BMPyrrOTf with conductivity value reaches upto 4.15×10^{-5} S/cm at. Using Wagner's polarization method, Ionic transferance measurement support ionic conduction while stable potential window has further affirmed good electrochemical stability of films. The highest conducting IL-enriched polymer electrolyte sandwiched low-cost dye-sensitized solar cells (DSSCs) and electric double layer capacitors (EDLCs) have been developed, and their performance is conveniently appropriate.

Address correspondence to E-mail: rawatsuneyana@gmail.com; pramodkumar.singh@sharda.ac.in; rcsingh@sharda.ac.in

<https://doi.org/10.1007/s10854-024-13397-4>

Published online: 27 August 2024

 Springer

1 Introduction

It is anticipated that renewable energy sources, such as solar-oriented cells, which convert solar energy into energy, will be able to provide humanity with endless energy [1]. In light of these problems, solar energy is one of the best possibilities because to its affordability, accessibility, security, and cleanliness, which enable the era of energy in remote rural places and promise future energy resources [2]. Photovoltaic cells are particularly interesting because they are among the most efficient renewable energy sources and are capable of converting daylight into electricity [3, 4]. They also offer several advantages over most current electrical control producing procedures. Other intriguing characteristics of the solar energy-oriented cell include its endless supply, requirement for further natural pollution, requirement for depletion that emits neonatal gases, and lack of atomic waste spinoffs [5]. The European Joint Research Centre projected that by 2050, 20% of all energy consumed would originate directly from solar energy, with the possibility of this percentage rising to above 50%. Generally speaking, a sun-powered cell is a device that uses the sun's limitless supply of pure energy to convert solar light energy into electrical energy [6]. Moreover, mechanical development or mobile components are not needed for electrical speculate cells to generate electricity [7]. The concept of charge division at a hetero-junction, or single intersection, between two completely different types of semiconductors (N and p-type) or semiconductor–metal (Schottky) junctions [8]. Solar energy based cells will therefore continue to function continuously without assistance and for a longer period of time than specific control technology progresses [9].

Polymer electrolytes are polymer compositions combined with salts [10]. When a polymer comes into contact with charged particles, its main chain's polar group can aid in their dissolution. To enable a material called a polymer conduct electricity, ions travel through its gaps. In 1973, researchers found that combining polyethylene oxide (PEO) with Nascent salt enables effective devices with energy storage, such solar panels and rechargeable batteries [11]. Other practical energy storage technologies including supercapacitors, fuel cells, and electrochromic windows were developed as a result of this finding. This essay discusses a 1978 study paper that Armand and associates wrote. Classical polymer electrolytes come in

various varieties, such as ionic rubber, gel, plasticized, and ion-conducting polymeric materials [12].

Ionic liquids, often known as ILs in simple terms, are a special kind of liquid substances that are made completely of ions. Ionic liquids are composed of positively charged (cations) and negatively charged (anions) species in contrast to conventional liquids, which are frequently made of molecules with neutral charges [13]. Due to the strong electrostatic forces holding these ions together, a liquid with distinctive properties and a wide range of uses is generated. Ionic liquids (ILs) have a fascinating heritage that dates beyond to over a century ago. The first room-temperature ionic liquid, ethyl ammonium nitrate, was created in 1914 by German scientist Paul Walden, which is when the idea of ionic liquids originated. But the phrase "ionic liquid" had not yet been created at that point. Ionic liquids can operate at an extensive range of voltages without experiencing substantial degradation because they generally have a large electrochemical window [14]. Particularly in high-voltage applications such as lithium-ion batteries, this attribute is crucial. Ionic liquids have the capacity to improve the polymer electrolyte's thermal stability, enabling the device to function at greater temperatures without experiencing a change in condition. Since ionic liquids are often non-volatile, there is less chance of fire dangers and electrolyte leaks, especially in high-temperature applications [15].

Ionic liquids (IL), known for their distinctive characteristics such as low volatility, a broad electrochemical stability window and highly effective thermal stability, are combined into polymer matrices to form evolved electrolytes [16]. In polymer electrolytes, ionic liquids are utilized to increase ionic conductivity and boost the electrolyte's overall performance [17]. Ionic salts and a polymer matrix are incorporated to generate materials known as polymer electrolytes, which are solid or gel-like substances that conduct ions [18]. They are utilized in a number of electrochemical systems, including as fuel cells, supercapacitors, and batteries [19]. There are several benefits of adding ionic liquids to polymer electrolytes. Ionic liquids have the potential to greatly increase polymer electrolytes' ionic conductivity which is already reported in the literature [20]. This is essential for the effective operation of electrochemical devices because more rapidly ion transport and improved device performance are made attainable by increased conductivity.

In this research article, an attempt has been tried to develop a new ionic liquid-doped polymer electrolyte

system. In our knowledge this particular system is not existed in literature. A wide variety of characterization tools discussed to evaluate their structural, electrical and optical properties in detail.

2 Experiment work

2.1 Electrolyte preparation

In a common preparation for solid polymer electrolyte films (solution casting method), ammonium iodide (NH_4I , Aldrich) and Polyethylene Oxide (PEO, Molecular weight = 10^5 , Aldrich) were dissolved in acetonitrile and rapidly stirred overnight to create a homogenous solution of polymer-salt electrolyte. For IL-doped polymer electrolyte, stoichiometric ratio of IL (in different wt%) was added in homogenous solution of polymer-salt electrolyte. These films were finally casted in polypropylene petri dishes at ambient temperature to get free standing IL-doped solid polymer electrolyte. Followed by vacuum drying (completely evaporate of residual solvent) films were then characterized using various characterization tools.

2.2 Electric double layer capacitor fabrication

$1 \times 1 \text{ cm}^2$ area of graphite sheet is used as the current collector in the fabrication of an EDLC. Conducting porous carbon paste made from waste plastic material [21] (reported by our group) utilized as the EDLC symmetrical electrodes. To create a homogenous mixture, thoroughly combine conductive porous activated carbon with a (PVFF-HFP) binder in a 9:1 using a pestle and mortar and mixed in acetone media. After coating it onto the graphite sheet surface (current collector) with a prepared mixture of porous carbon (1 mg/ cm^2 paste), the sheet was dried overnight at $90 \text{ }^\circ\text{C}$ in an oven. In order to fabricate the super capacitor, the optimized PEO: NH_4I :IL polymer electrolyte was positioned between the porous activated carbon electrode

as shown in Fig. 1. Since polymer electrolyte film itself sticky in nature we do not taken any extra precautions.

2.3 Dye-sensitized solar cells fabrication

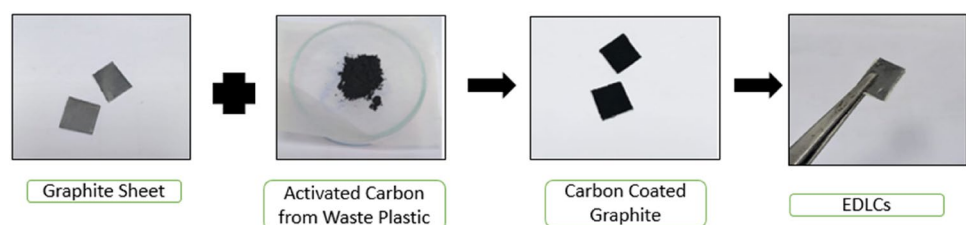
To fabricate a DSSC with area ($2.5 \times 2.5 \text{ cm}^2$), pieces of conducting FTO (fluorine-doped tin oxide) glass was thoroughly cleaned with solution of acetone and distilled water (1:1). The FTO glass is then coated with a light layer of $\text{C}_{16}\text{H}_{32}\text{O}_6\text{Ti}$ (titanium diisopropoxide bisacetylacetonate), as a blocking layer onto FTO by spin coating method, and then it is tempered for 30 min at $500 \text{ }^\circ\text{C}$. Using doctor blade technique, transparent titanium di oxide (TiO_2 , purchase from Solaronix, Switzerland) paste was coated over the blocking layer and annealed at $500 \text{ }^\circ\text{C}$ for 30 min. This TiO_2 coated electrode was then dipped in N_3 -dye solution for over 5–7 h, for successful fabrication of working electrode [22]. Similarly, the counter electrode prepared utilizing the cleaned FTO conducting glass whereby applied platinum acid solution using spin coating, which is then tempered at $500 \text{ }^\circ\text{C}$ in furnace for 30 min. In order to the fabricate DSSC, PEO: NH_4I :IL polymer electrolyte film (maximum conductivity) between a prepared working electrode and a counter electrode as shown in Fig. 2.

3 Results and discussion

3.1 X-ray diffraction (XRD)

The X-ray patterns of PEO: NH_4I complex and PEO: NH_4I doped with 8, 10 wt% ionic liquid are shown in Fig. 3. PEO: NH_4I spectra shows well defined three semi crystalline peaks at 2θ , values of 23.24, 26.15, 26.91, respectively. Adding IL into PEO: NH_4I matrix, it was noticed that peaks intensity goes down along with broadening in peaks occur. These observation clearly confirms that with doping IL crystallinity reduces the crystalline matrix of polymer electrolyte

Fig. 1 Schematic diagram for fabrication of EDLC



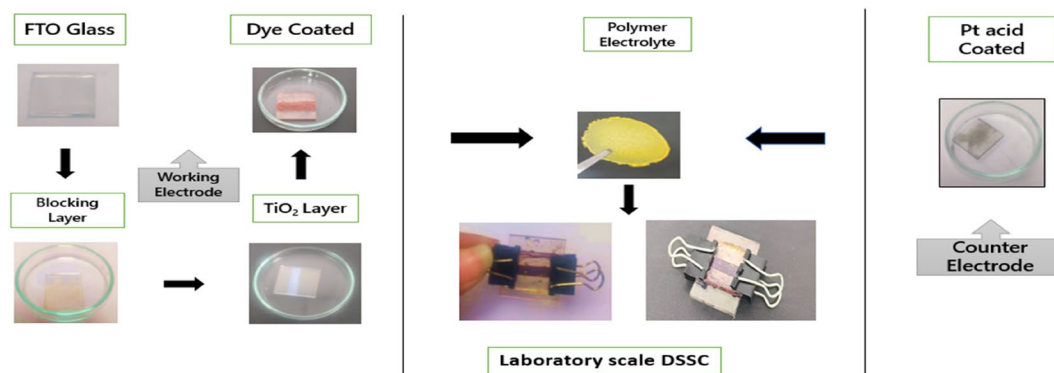


Fig. 2 Laboratory scale fabrication of dye-sensitized solar cell

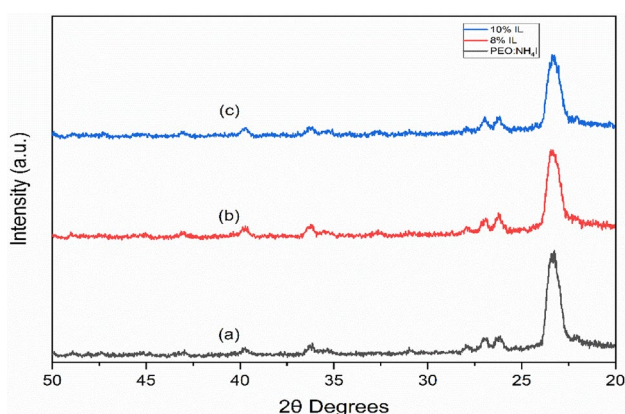


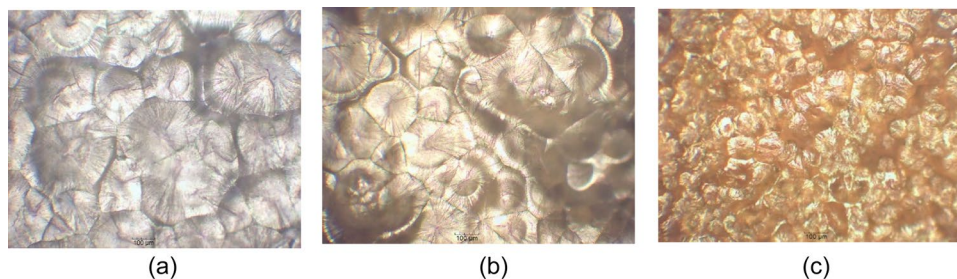
Fig. 3 X-ray diffraction patterns of **a** PEO: NH_4I and PEO: NH_4I doped with **b** 8 wt% and **c** 10 wt% of ionic liquid

and provide more amorphous nature which is certainly assist in ion movement within polymer matrix and hence conductivity enhances.

3.2 Polarizing optical microscopy

Polarized optical micrographic (POM) images of pure PEO, PEO: NH_4I , and IL-doped PEO: NH_4I polymer electrolytes are obtained at $\times 10$ magnification (Mote

Fig. 4 POM image of pure PEO **(a)**, PEO doped with NH_4I **(b)** and **c** PEO + NH_4I + IL polymer electrolyte films



Model no. 3A310 pol, Carlsbad, CA, USA). It is reveal that the pure PEO polymer film (Fig. 4a) displays a pure semi crystalline that is generously sized and spherical, with firmly packed spherulites while infusing of NH_4I into the polymer host (Fig. 4b) resulted size decreases as well as increase in amorphous region which appears as black portion in POM. It was also observed that the amorphous region increases continuously upon adding IL into the polymer-salt complex. PEO: NH_4I :IL polymer electrolyte matrix provides a further rise in amorphicity, where the blackish, highly dense region increases vis a vis decrease in spherulites size significantly observed as shown in (Fig. 4c).

This observation again affirms our phenomenon which we have already explain in Sect. 3.1.

3.3 Fourier transform infrared spectroscopy (FTIR)

Complexation (interaction with polymer and ions) and for composite nature we have examined this phenomenon by recording different FTIR spectra using FTIR spectrometer (CARY 630, AGILENT, California). The FTIR peaks which recorded in the transmittance mode and then converted into absorbance mode between wavenumber 600 and 3500 cm^{-1} at room environment.

Prior to every sample run's IR spectrum acquisition, background spectrum was captured for levelling and smoothness of spectra's. The FTIR spectrum of PEO, NH_4I , $\text{PEO:NH}_4\text{I}$ and $\text{PEO:NH}_4\text{I:IL}$ polymer electrolyte films are recorded and shown in Fig. 5. All corresponding peaks assignments for particular bonding and their nature are shown in Table 1.

From Table 1 and Fig. 5, it was clear that there is close interaction between polymer (PEO) and salt (NH_4I) or IL. In case of electrolyte $\text{PEO:NH}_4\text{I}$ as observed in Table 1(a), (b) and (c) it appears as in the form of the shifting of FTIR bands. Doping IL into $\text{PEO:NH}_4\text{I}$, depicts same phenomenon observed as as obverse in Table 1(d), (c) and (e). Additionally, it has been found that IL-doped $\text{PEO:NH}_4\text{I}$ system contains peaks either from Polymer, salt or IL, i.e. no new peaks appear in ionic liquid-doped polymer electrolyte system which confirms composite characteristic of these IL-doped polymer electrolyte system [18–27].

3.4 Electrical impedance analysis

Complex impedance spectroscopy was used to measure the ionic conduction of PEO, PEO complexed with NH_4I , and IL (1-Butyl-1-Methylpyrrolidinium Trifluoromethanesulfonate)-doped $\text{PEO:NH}_4\text{I}$ by recording the real (Z or Z') and imaginary (Z'') to assessed bulk resistance. The main metric used to evaluate the ionic conductivity of the electrolytic system is bulk resistance, likewise known as electrolyte resistance. One might quickly ascertain the total resistance

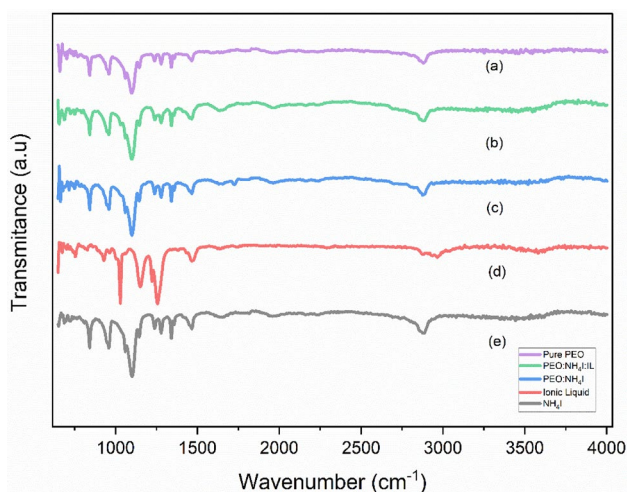


Fig. 5 FTIR spectrum of (a) PEO film, (b) $\text{PEO:NH}_4\text{I:IL}$ matrix, (c) $\text{PEO:NH}_4\text{I}$, (d) IL (e) NH_4I

of an ionic conducting system by applying Ohm's law. However, ion conducting systems are more difficult to compute since ions deposited at the interface between the electrode and the electrolyte increase their resistance when exposed to DC potential. Between 10^6 and 10^2 Hz, a high-frequency alternating current was run between the electrodes. The bulk resistance is determine using the Nyquist graph shown in Fig. 6. The ionic conductivity of the solid polymer electrolyte films is evaluated by Eq. (1).

$$\sigma = \frac{l}{RbA} \quad (1)$$

where "A" is the area that comes in contact with the polymer electrolyte, "l" is the thickness of the electrolytic layer, and "Rb" is the bulk resistance.

We have evaluated the conductivity value using Eq. 1 and values are given in table while graphical presentation of conductivity vs composition of IL is shown in Fig. 7. In PEO complexed with NH_4I (80:20 wt%) shows conductivity maxima with conductivity value 3.34×10^{-8} S/cm. This value is cross verified with data reported in literature [37–39]. From Fig. 7 and Table 2, it is clear that the doping ionic liquid in polymer electrolyte increases ionic conductivity sharply attain maxima and then decreases. In present system we attain maxima at 8wt% ionic liquid concentration where conductivity value reaches up to 4.15×10^{-5} S/cm. and subsequently goes down. It is in literature that single or double maxima in these polymer electrolytes could be explain in term of enhancement in number of mobile charge carriers (n) or mobility of ions within polymer matrix or ease/fast movement of ions in less crystalline (more viscous) polymer electrolyte matrix as govern by Eq. 2 given below

$$\sigma = nq\mu \quad (2)$$

where q is columbic charge, n is the number of mobile charge carriers, μ is mobility of charge carriers. Furthermore σ decrease is also cited in literature as charge carriers ion pair formation or hinders of mobile charge carriers [40].

3.4.1 Ionic transference number t_{ion}

3.4.1.1 Wagner's polarization method The ionic transference number (t_{ion}) is calculated to ascertain whether the IL-doped polymer electrolyte is ionic or electronic. Wagner's polarization technique is used to compute

Table 1 FTIR peak assignments for Pure PEO, NH₄I, PEO:NH₄I and PEO:NH₄I:IL polymer electrolyte films

Component	Wavenumber (cm ⁻¹)	Peak assignment	Class	Ref.	
PEO (a)	3391	Stretching O–H asymmetric	Alcohol	[23]	
		N–H Stretching	Secondary Amine		
	2879	Stretching C–H	Alkane	[24]	
	1466	Stretching C–H	Alkane	[25]	
	1338	C–H Bending	Alkane		
	1276	C–O Stretching	Aromatic ester	[26]	
		C–N Stretching	Aromatic amine		
	1098	Stretching C–O	Secondary alcohol	[24]	
	960	C=C Bending	Alkene	[27]	
	841	Stretching C–Cl	Halo Compound	[26]	
	NH ₄ I (b)	2880	O–H Stretch	Carboxylic acid	[28]
			O–H Stretch	Alcohol	
			N–H Stretch	Amine	
		C–H Stretch	Alkane		
1469		bending C–H	Alkane	[29]	
1346		Bending O–H	Alcohol	[30]	
1104		C–O Symmetric stretching	Secondary alcohol	[31]	
1083		stretching C–O	Primary Alcohol	[32]	
842		stretching C–Cl	Holo Compound	[24]	
Ionic Liquid (d)		2965	Stretching O–H	Carboxylic acid	[24]
		Stretching N–H	Amine Salt		
	2880	Stretching C–H	Alkane	[24]	
	1466	Stretching C–H	Alkane	[24]	
	1256	Stretching C–F	Fluoro compound	[24]	
		Stretching C–O	Alkyl aryl ether		
	1151	Stretching C–O	Tertiary Alcohol	[24]	
	1028	Stretching C–F	Fluoro compound	[24]	
	775	Stretching C–H	Halo compound	[24]	
		Bending C–H	1,2, Disubstituted		
	PEO:NH ₄ I (c)	2877	Stretching O–H	Alcohol	[33]
1466		Stretching C–H	Alkane	[24]	
1341		Bending C–H	alcohol	[24]	
1279		Stretching C–F	Fluoro compound	[24]	
		Stretching C–N	Aromatic Amine		
1099		Stretching C–F	Fluoro compound	[31]	
		Stretching C–O	Secondary alcohol		
959		C–C, C–O deoxyribose		[34]	
847		Stretching CH	Halo Compound	[35]	
PEO:NH ₄ I:IL (e)		2884	Stretching C–H	–	[28]
	1469	PO ₂ ⁻ asymmetric	–	[32]	
	1346	CH ₂ wagging	–	[30]	
	1280	Symmetric stretching P–O–C	–	[31]	
	1099	PO ₂ ⁻ asymmetric	–	[32]	
	842	C–Cl stretching	Halo Compound	[35]	
	983	OCH ₃ (polysaccharides-cellulose)	–	[36]	

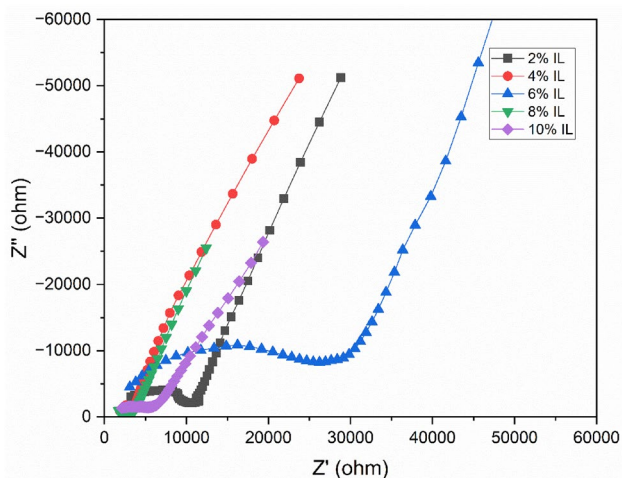


Fig. 6 Impedance plots of composition of IL in PEO:NH₄I polymer electrolyte matrix

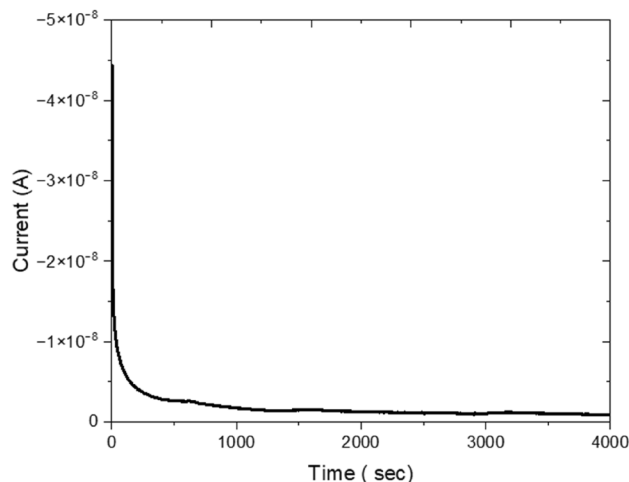


Fig. 8 Time vs current curve to evaluate t_{ion} in maximum conducting IL-doped polymer electrolyte

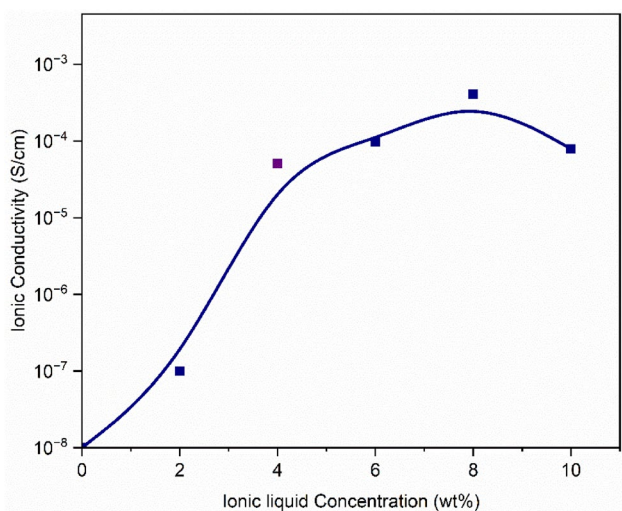


Fig. 7 Ionic liquid concentration vs conductivity plot in IL-doped PEO:NH₄I polymer electrolyte system

Table 2 Ionic conductivity of IL-doped PEO:NH₄I polymer electrolyte system

Ionic liquid concentration (wt%)	Ionic conductivity (S/cm)
0%	3.34×10^{-8}
2%	8.70×10^{-7}
4%	4.38×10^{-6}
6%	8.79×10^{-6}
8%	4.15×10^{-5}
10%	3.09×10^{-6}

Conductivity maxima is given in bold

the ionic transference number where current flow causes the electrode potential to deviate from its equilibrium condition, this is referred to as polarization in electrochemical systems. The measurement of a system’s resistance to this variance may be used to infer the electrochemical behaviour of the system from the polarization resistance. The Wagner’s Polarization technique involves applying a small DC voltage to the electrochemical system and measuring the current response that results. Typically, a short amount of voltage supply is used to allow the current to stabilize. The voltage and current parameters are then used to calculate the polarization resistance using Eq. 3

$$t_{ion} = \frac{\text{Initial Current} - \text{Final Current}}{\text{Initial Current}} \quad (3)$$

The initial current in the current vs. time plot is the entire current contributed by both electrons and ions, while the continuous residual current is solely the result of electronic current. It is in literature that salt-doped polymer system shows nearby 0.9 to 0.98 value which depicts that these systems are predominantly govern by ions only. For IL-doped polymer electrolyte system we have chosen a typical maximum ionic conducting system. Time vs Current plot is shown as Fig. 8, we have evaluated t_{ion} value which comes to 0.98 which clearly affirm that IL-doped polymer electrolyte system are due to ions only.

3.5 Linear sweep voltammetry

Using a linear sweep voltammeter, the voltage window for electrochemical stability is assessed. The highest conductive polymer electrolyte, which is placed between two stainless steel electrodes, undergoes exposure to a voltage between -3 and 3 V in order to detect the voltage. Figure 9 shows that the system started oxidizing at -0.77 V and reduced at 2.25 V when 10 mV/s is applied across the polymer electrolyte layer, in accordance with the literature. Furthermore, the IL-doped polymer electrolyte has an ESW value of 3.32 V, which qualifies its suitability for use in the development of electrochemical devices [41].

3.6 EDLC performance

3.6.1 Cyclic voltammetry

Sandwiched structure EDLCs have been fabricated using symmetric electrodes coated with carbon and maximum conducting IL-doped polymer electrolyte. To evaluate specific capacitance the cyclic voltammetry (CV) of the fabricated EDLC was measured at two scan rates of 50 mV/s and 5 mV/s for more accuracy on -1 to 1 Voltage. The hysteresis curve of a cyclic voltammetry shows the standard behaviour of super capacitor. The super capacitor cell's specific capacitance has been measured quantitatively using Eq. 4

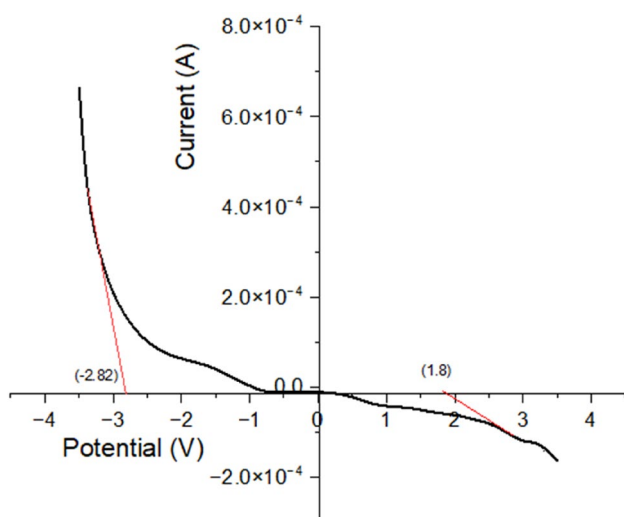


Fig. 9 Linear sweep voltammeter (LSV) plot between potential Vs current of one typical maximum conducting IL-doped polymer electrolyte

$$C_{sp} = \frac{1}{m \times s \times \Delta v} \int_{v_1}^{v_2} I(v) dv \quad (4)$$

where m is the mass of active material at a single electrode, Δv is the potential difference between the initial (v_1) and final (v_2) voltage range, s is scan rate, and integral part is the area enclosed in CV from Fig. 10. Evaluation of the specific capacitance values found 16.5 F/gm at 50 mV/s and 87.8 F/gm at 5 mV/s, respectively.

3.7 DSSC performance

3.7.1 J-V characterization

Using maximum conducting ionic liquid-doped polymer electrolyte and FTO coated electrodes we have fabricated dye-sensitized solar cells (DSSC) with active area 0.95 cm². For DSSC efficiency, we have used solar simulator (model no-SS-F5-3A, company- Enlitech, Taiwan) situated in our laboratory. Different parameters of DSSC was carried out using following equations

$$FF = \frac{V_{max} \times J_{max}}{V_{oc} \times J_{sc}} \quad (5)$$

$$\eta = \frac{V_{oc} \times J_{sc}}{P_{in} \times FF} \quad (6)$$

where FF is represented by fill factor, V_{max} is maximum voltage, J_{max} is maximum current, η is efficiency of the solar cell by conversion of photon into electrical

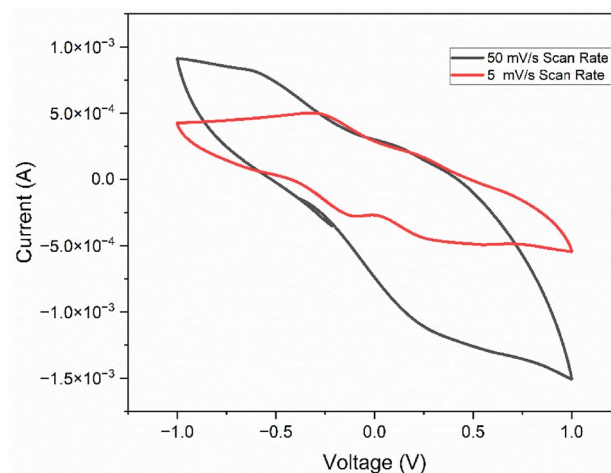
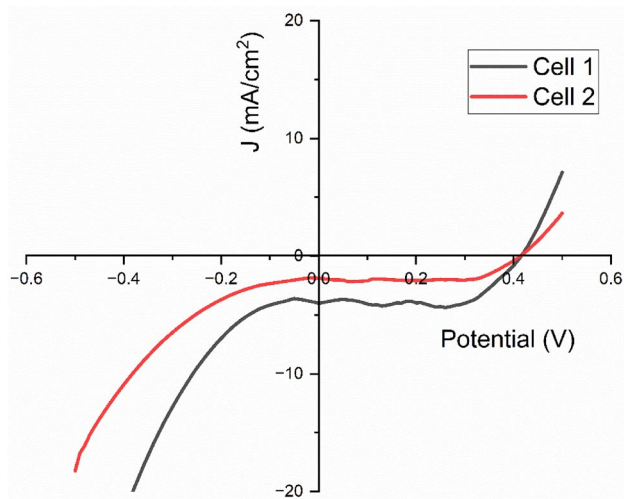


Fig. 10 Cyclic voltammetry curve of fabricated sandwich EDLC at 5 mV and 50 mV scan rate

Table 3 DSSC parameters of developed dye-sensitized solar cell at 1 sun condition

Name	I_{sc} (mA)	V_{oc} (V)	Efficiency (%)	Fill factor (%)	J_{sc} (mA/cm ²)
Cell 1	0.51	0.46	1.30	54.14	5.18
Cell 2	0.40	0.41	1.19	71.96	4.00

**Fig. 11** J - V characteristics recorded at 1 sun condition for fabricated DSSCs (cell 1, 2)

energy. The recorded J - V curve for sandwich DSSC using maximum conducting IL-doped solid polymer electrolyte is shown in Fig. 9. Using Eqs. (5) and (6) we have calculated parameters and parameters are listed in Table 3. The fabricated solar cell shows stable efficiency of 1.30% at 1 sun condition. Furthermore, to check cell life we have placed our cell in room environment condition. Our solar cells are alive till more than 6 months with reasonable deterioration in J_{sc} and V_{oc} (Fig. 11).

4 Conclusion

In this paper, Polyethylene oxide (PEO)-doped ammonium iodide (NH_4I) has been prepared. To achieve further enhancement in conductivity an ionic liquid has been doped and a high conducting IL-doped solid polymer electrolyte has been synthesized and characterized using various experimental tools like XRD, POM, FTIR and complex impedance spectroscopy. XRD and POM suggest reduction in crystallinity by IL doping while FTIR confirm good complexation and composite

nature. Impedance spectroscopy affirm that doping of IL provide more amorphous matrix/more free ions. In amorphous matrix it is documented that ion movement is easy and fast and hence conductivity increases by IL doping. The voltage window for electrochemical stability is calculated by LSV is 3.32 V which affirm its suitability towards electrochemical application. Using maximum conducting IL-doped polymer electrolyte we have designed sandwich-structured EDLC and DSSC. The fabricated EDLC shows specific capacitance of 87.8 F/gm at 5 mV/S while developed DSSC shows stable 1.30% efficiency at 1 sun conduction.

Acknowledgements

We are thankful to the CSTUP (CST/D-1041), Lucknow, Govt. of India for the financial support for research work.

Author contributions

To this manuscript, each author has contributed equally.

Data availability

On request, the corresponding author will provide the data supporting the study's conclusions. The statistics are not accessible to the general public because of concerns regarding privacy and ethics.

Declarations

Conflict of interest There are no conflicts of interest to disclose.

References

1. H. Meddeb, M. Götz-Köhler, N. Neugebohrn, U. Banik, N. Osterthun, O. Sergeev, D. Berends, C. Lattiyak, K. Gehrke, M. Vehse, *Adv. Energy Mater.* **12**, 2200713 (2022)
2. K. Ukoba, K.O. Yoro, O. Eterigho-Ikelegbe, C. Ibegbulam, T.-C. Jen, *Heliyon* **10**, e28009 (2024)
3. G.T. Chala, S.M. Al Alshaikh, *Energies* **16**, 7919 (2023)

4. E.K. Solak, E. Irmak, RSC Adv. **13**, 12244 (2023)
5. M. Coccia, Sustain. Futures **5**, 100114 (2023)
6. European Commission. Joint Research Centre, *Towards Net-Zero Emissions in the EU Energy System by 2050: Insights from Scenarios in Line with the 2030 and 2050 Ambitions of the European Green Deal* (Publications Office, LU, 2020)
7. J. Tan, X. Wang, W. Chu, S. Fang, C. Zheng, M. Xue, X. Wang, T. Hu, W. Guo, Adv. Mater. **36**, 2211165 (2024)
8. C.V. Prasad, J.H. Park, J.Y. Min, W. Song, M. Labed, Y. Jung, S. Kyoung, S. Kim, N. Sengouga, Y.S. Rim, Mater. Today Phys. **30**, 100932 (2023)
9. M. Ashraf, M. Ayaz, M. Khan, S.F. Adil, W. Farooq, N. Ullah, M. Nawaz Tahir, Energy Fuels **37**, 6283 (2023)
10. V. Nain, H.S. Shyam, D. Gupta, S. Singh, Macromol. Symp. **413**, 2300091 (2024)
11. Z. Gu, X. Xin, M. Men, Y. Zhou, J. Wu, Y. Sun, X. Yao, Batter. Supercaps **6**, e202300267 (2023)
12. A.G. Chaudhary, A. Vashisht, H.S. Shyam, A.S. Malhi, R. Gupta, Macromol. Symp. **413**, 2300092 (2024)
13. S.M.S. Hussain, A.A. Adewunmi, O.S. Alade, M. Murtaza, A. Mahboob, H.J. Khan, M. Mahmoud, M.S. Kamal, J. Taiwan Inst. Chem. Eng. **153**, 105195 (2023)
14. Z. Lei, C. Dai, J. Hallett, M. Shiflett, Chem. Rev. **124**, 7533 (2024)
15. S.K. Singh, A.W. Savoy, J. Mol. Liq. **297**, 112038 (2020)
16. T. Zhou, C. Gui, L. Sun, Y. Hu, H. Lyu, Z. Wang, Z. Song, G. Yu, Chem. Rev. **123**, 12170 (2023)
17. S. Nazir, S.P. Pandey, F.A. Latif, P.K. Singh, Macromol. Symp. **413**, 2300035 (2024)
18. G. Skorikova, D. Rauber, D. Aili, S. Martin, Q. Li, D. Henskensmeier, R. Hempelmann, J. Membr. Sci. **608**, 118188 (2020)
19. H.S. Shyam, I. Shuaib, S.P. Pandey, Macromol. Symp. **407**, 2200068 (2023)
20. S. Rawat, P.K. Singh, S.P. Pandey, R.C. Singh, Macromol. Symp. **413**, 2300050 (2024)
21. S. Pandey, M. Karakoti, K. Surana, P.S. Dhapola, B. SanthiBhushan, S. Ganguly, P.K. Singh, A. Abbas, A. Srivastava, N.G. Sahoo, Sci. Rep. **11**, 3916 (2021)
22. P.K. Singh, U. Singh, B. Bhattacharya, H.-W. Rhee, J. Renew. Sustain. Energy **6**, 013125 (2014)
23. C. Zhu, H. Cheng, Y. Yang, J. Electrochem. Soc. **155**, A569 (2008)
24. S.A. Khan, S.B. Khan, L.U. Khan, A. Farooq, K. Akhtar, A.M. Asiri, in *Handbook of Materials Characterization*. ed. by S.K. Sharma (Springer, Cham, 2018), pp.317–344
25. J. Spěváček, R. Konefař, J. Dybal, E. Čadová, J. Kovářová, Eur. Polym. J. **94**, 471 (2017)
26. N. Rakkapao, V. Vao-soongnern, Y. Masubuchi, H. Watanabe, Polymer **52**, 2618 (2011)
27. L.J. Bellamy, in *The Infrared Spectra of Complex Molecules*. (Springer, Dordrecht, 1980), pp.24–58
28. T. Glaser, C. Müller, M. Sendner, C. Krekeler, O.E. Semonin, T.D. Hull, O. Yaffe, J.S. Owen, W. Kowalsky, A. Pucci, R. Lovrinčić, J. Phys. Chem. Lett. **6**, 2913 (2015)
29. M.A. Ben Abdallah, J. Mol. Struct. **1171**, 76 (2018)
30. K.M. Harmon, J.A. Bulgarella, J. Mol. Struct. THEOCHEM **377**, 155 (1996)
31. H.T. Ahmed, O.Gh. Abdullah, Results Phys. **16**, 102861 (2020)
32. Y. Long, X. Dong, L. Huang, H. Zeng, Z. Lin, L. Zhou, G. Zou, Mater. Today Phys. **28**, 100876 (2022)
33. C. Branca, G. D'Angelo, C. Crupi, K. Khouzami, S. Rifici, G. Ruello, U. Wanderlingh, Polymer **99**, 614 (2016)
34. P.J. Gomes, P.A. Ribeiro, D. Shaw, N.J. Mason, M. Raposo, Polym. Degrad. Stab. **94**, 2134 (2009)
35. C. Rauch, A. Pichler, M. Trieb, B. Wellenzohn, K.R. Liedl, E. Mayer, J. Biomol. Struct. Dyn. **22**, 595 (2005)
36. K. Sommer, C. Zollfrank, Biomacromol **23**, 2280 (2022)
37. R.T. Abdulwahid, S.B. Aziz, M.F.Z. Kadir, J. Phys. Chem. Solids **167**, 110774 (2022)
38. P.K. Singh, S. Chandra, A. Chandra, J. Mater. Sci. Lett. **21**, 1393 (2002)
39. S. Singh Negi, S. Rawat, P.K. Singh, S.V. Savilov, T. Yadav, M.Z.A. Yahya, R. Chandra Singh, ChemistrySelect **9**, e202400847 (2024)
40. N. Lakshmi, S. Chandra, Bull. Mater. Sci. **25**, 197 (2002)
41. S.B. Aziz, E.M.A. Dannoun, A.R. Murad, K.H. Mahmoud, M.A. Brza, M.M. Nofal, K.A. Elsayed, S.N. Abdullah, J.M. Hadi, M.F.Z. Kadir, Alex. Eng. J. **61**, 5919 (2022)

Publisher's Note Springer Nature remains neutral with regard to jurisdictional claims in published maps and institutional affiliations.

Springer Nature or its licensor (e.g. a society or other partner) holds exclusive rights to this article under a publishing agreement with the author(s) or other rightsholder(s); author self-archiving of the accepted manuscript version of this article is solely governed by the terms of such publishing agreement and applicable law.